

Saturation spectroscopy and velocity-selective optical pumping of oxygen using an (Al,Ga)As diode laser

M. de Angelis,* M. Inguscio,[†] L. Julien,[‡] F. Marin,[§] A. Sasso,* and G. M. Tino*

European Laboratory of Nonlinear Spectroscopy (LENS), largo Enrico Fermi 2, I-50125 Firenze, Italy

(Received 19 February 1991; revised manuscript received 8 July 1991)

Saturation spectroscopy, velocity-selective atomic orientation, and velocity-selective alignment have been applied to a high-resolution investigation of the $3s^5S_2-3p^5P_{1,2,3}$ transitions at 777 nm of atomic oxygen. Pure Lorentzian lineshapes were obtained, which allowed an accurate measurement of the radiative linewidth. Using an isotopically enriched sample, isotope shifts and hyperfine structure were resolved and measured.

PACS number(s): 32.30.Jc, 35.20.Sd, 32.80.Bx, 32.70.Jz

I. INTRODUCTION

In a recent Letter [1], we reported the results of a measurement of the hyperfine structure of an optical transition of atomic oxygen. In that experiment, a narrow-linewidth $\text{Al}_x\text{Ga}_{1-x}\text{As}$ diode laser was used to perform saturation spectroscopy, which allowed us to resolve sub-Doppler spectral features. As mentioned in that paper, the interest of measuring nucleus-dependent effects in the spectrum of oxygen arises from the particular structure of the ^{16}O nucleus, which is "doubly magic," having both proton and neutron closed shells. In fact, a nuclear size contribution to the observed isotope shift in optical transitions has been evidenced [2], although for such light atoms this effect is usually absolutely negligible. Other important information which can be extrapolated from the sub-Doppler data is relative to the lifetime of the upper level of the investigated $3s^5S_2-3p^5P_3$ transition (Fig. 1). This level is involved in a scheme which

has been proposed for the cooling of atomic oxygen in its ground state, and the estimated radiative lifetime supported the proposal of this new cooling scheme [1]. More recently, this transition has been recorded in natural oxygen by means of optogalvanic saturation spectroscopy [3], in the frame of an investigation of anomalously broadened line shapes [4].

In the present paper we report the results of more accurate and extensive measurements of the hyperfine structure of the $3s^5S_2$ level and of the just-mentioned $3p^5P_3$ lifetime. Also, accurate values for the ^{16}O - ^{18}O isotope shift and for the fine structure of the $3p^5P_{1,2,3}$ level are given. Different high-resolution techniques have been used: saturation spectroscopy, velocity-selective atomic orientation, and velocity-selective atomic alignment. As far as hyperfine structure and isotope shift are concerned, the different techniques give, of course, results in agreement with each other. However, the intensity and shape of the lines depend on the relevant physical observable and on the effect of collisions on the signal. A comparison of the different techniques allowed us to optimize the experimental parameters depending on the specific quantity to be measured.

II. COLLISIONAL LINE SHAPES IN SATURATION SPECTROSCOPY AND VELOCITY-SELECTIVE OPTICAL PUMPING

The three techniques used in this work, namely saturation, velocity-selective orientation, and velocity-selective alignment, correspond to the study of three different observables; they are, respectively, the level population, the atomic orientation, and the atomic alignment. As will be shown in the following, the main advantage offered by the techniques based on velocity-selective optical pumping [5], compared to pure saturation spectroscopy, was the reduction of the broadening due to collisions and the resulting improvement in spectral resolution. However, when in the presence of fine or hyperfine structures, a complication of the spectra can arise. In fact, saturation spectroscopy resonance signals always have the same sign

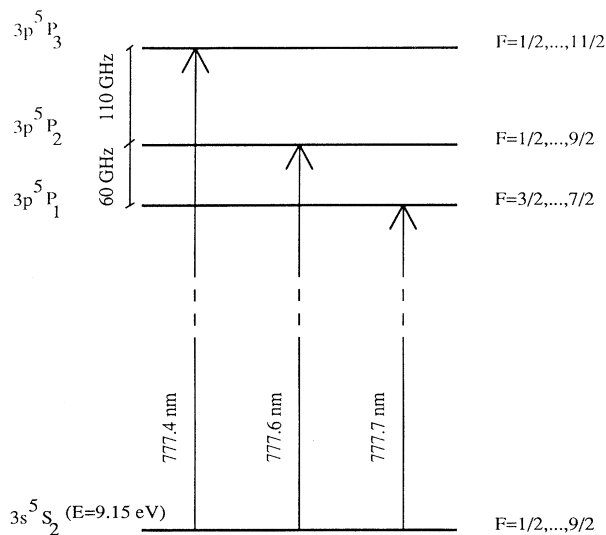


FIG. 1. Partial scheme of the energy levels of atomic oxygen with the transitions investigated in the present work. Wavelengths are *in vacuo*.

and crossover resonances appear only when close-by transitions are present, sharing a common level. On the contrary, in optical pumping where stimulated emission is negligible, both positive and negative signals can be observed; also, crossover resonances arise for transitions without common levels [6].

The optical pumping signals depend on the collisional depolarization of the states involved in the transition. Generally at low pressures no such collisions occur during the lifetime τ of the upper level: This is the “Kastler type” optical pumping scheme [7].

The situation is different if the pressure is high enough, so that the mean free time for collisions is smaller than the lifetime of the excited state. In this case, most of the excited atoms undergo collisions before they decay. Collisions induce transfers between sub levels of the excited state. Optical pumping can still be obtained in this case, provided the atoms in the lower state are not disoriented in the collisions (Dehmelt scheme). For example, it has been shown [8] that collisions cannot disorient atoms in an S state, for which the magnetic moment is a pure spin moment. Instead, transfers between magnetic sub levels are possible if the atom is in a P or D state. Therefore, if the lower and upper states of a transition are an S and P state, respectively, optical pumping is possible; it depends only on the different rate at which the exciting light is absorbed by the sub levels of the lower level. In fact, as a result of collisions, excited atoms will return at an equal rate to all the sub levels.

For a complete understanding of the results presented in this paper, it is necessary to also consider another effect of collisions. It is well known in saturation spectroscopy that collisions can rethermalize the velocity distribution altered by the laser radiation; typically, this effect of what are called velocity-changing collisions (VCC) manifests itself in a broad background on which the homogeneous resonance signal is superimposed. VCC have been widely investigated, especially in saturation spectroscopy [9].

It is customary to divide VCC into “strong” and “weak” collisions; collisions are considered of the “strong” type when any memory of the initial velocity is lost after a single collision. In the hypothesis of a homogeneous width γ is much smaller than the Doppler width $\Delta\nu_D$, the line profile can be approximated by the superposition of a Lorentzian $L(\nu)$ (Doppler-free signal) and a Gaussian collisional pedestal $G(\nu)$

$$S(\nu) = A [L(\nu) + CG(\nu)] , \quad (1)$$

where S denotes signal, L has the width γ and G the width $\Delta\nu_D/\sqrt{2}$, A is a normalization constant, and C gives the weight of the collisional pedestal.

When, on the contrary, many collisions are required to change the atoms’ velocity, collisions are said to be “weak”; these collisions mainly lead to a broadening of the resonance peak.

VCCs may or may not depolarize atomic orientation and alignment; it depends on the depolarization cross section for the specific observable considered. The collisional background will be observed only when the observable

detected is not completely destroyed during collisions. Different line shapes can be expected, then, when observables corresponding to different multipole components are considered. The experimental line shapes are also expected to depend strongly on the collisional partners. For example, 5S oxygen atoms cannot be depolarized in collisions with noble gas atoms (Wigner’s spin conservation rule), while spin-exchange collisions between 5S atoms and O_2 molecules in the $^3\Sigma$ ground state have a large cross section [10]. In the former case, then, a much more intense background can be expected.

The presence of external fields can also influence the shape of spectral lines; for example, if orientation is being observed, the presence of a longitudinal magnetic field will tend to preserve the orientation of the atoms, giving rise to the background. An opposite effect has been observed [11] when the magnetic field is applied to the sample cell in a direction perpendicular to the circularly polarized laser beam. In this case, the oriented magnetic moments start precessing at the Larmor frequency and depolarization takes place. Of course, depolarization is more effective for atoms undergoing collisions; the background, which is produced by atoms whose velocity has been changed from v to $-v$ by one or more collisions, will then be depolarized in lower magnetic fields than the resonance. The pure Lorentzian line shape can be recovered in this way, which is particularly important in those cases where, as for the hyperfine structure measurements reported below, high resolution is required.

III. EXPERIMENTAL SETUP

The experimental setup is depicted in Fig. 2. The laser was a commercial $Al_xGa_{1-x}As/GaAs$ diode laser, mounted in an extended cavity configuration [1]. The 9-cm-long external cavity consisted of a collimating lens (numerical aperture=0.5), a 30% reflection beamsplitter, and a diffraction grating in the Littrow configuration. The grating was mounted on a piezoelectric transducer (PZT), in order to scan the length of the external cavity. The output power was ~ 6 mW in a single mode (jitter ~ 1 MHz). Coarse tuning was achieved by changing the temperature of the diode along with the grating angle. Frequency scans of ~ 10 GHz were accomplished by synchronously changing the length of the cavity and the injection current of the laser.

The calibration of the frequency scan was provided by a high-finesse Fabry-Pérot cavity with a free spectral range of 75 MHz. Care was required in positioning this cavity, as well as all the optical elements in the beam, in order to avoid undesirable optical feedback on the laser. A reduction of the sensitivity to this effect, however, was observed when the laser worked in the extended cavity configuration. The wavelength meter was a Michelson interferometer (constructed by R. Drullinger of NIST, Boulder, Colorado); the maximum achievable accuracy was 1 part in 10^7 . Generally, it was used to easily tune the laser frequency to the spectral lines of interest. In this experiment, its high accuracy was also exploited to measure the fine structure of the $3p^5P_{1,2,3}$ level of ^{16}O .

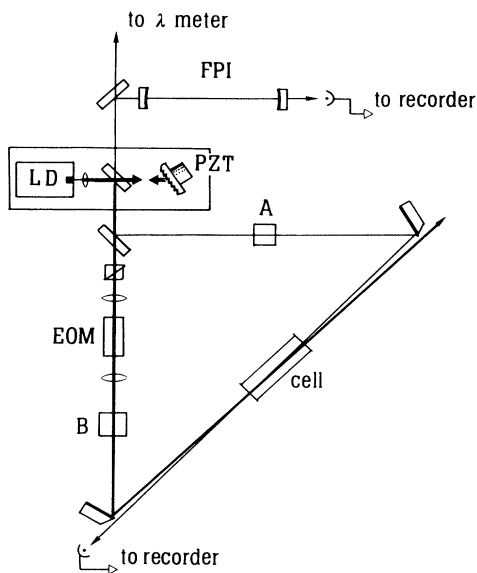


FIG. 2. Schematic diagram of the experimental apparatus. Optical feedback from a grating mounted on a piezoelectric transducer (PZT) allows us to control the frequency of the laser diode (LD). *A* and *B* indicate different optical devices depending on the detection technique (see text). FPI: Fabry-Pérot interferometer, EOM: electro-optic modulator.

The laser was locked on each of the three fine-structure components and its wavelength was measured. This was accomplished by introducing a 10 kHz modulation on the cavity length by means of the piezoelectric transducer on the grating; the laser frequency was then locked on the zero of the first derivative of the sub-Doppler saturation signal by feeding back the error signal, through an integrator, to the PZT.

The sub-Doppler signals were obtained by sending two counterpropagating beams (pump beam size $\sim 2.5 \times 6 \text{ mm}^2$) into the discharge cell. The polarization and modulation characteristics of the beams, however, were different depending on the observable of interest. In saturation spectroscopy, an electro-optic modulator (EOM) was used as a chopper for intensity modulation of the pump beam; in this case *A* and *B* (in Fig. 2) were linear polarizers. Modulation frequencies of about 6 kHz were used.

In the orientation modulation technique, instead, the EOM was square-wave modulated to give an alternate $\sigma^+ - \sigma^-$ polarization of the pump beam; here, *A* was a linear polarizer followed by a quarter-wave retarder while *B* was absent. Finally, for the alignment detection, the EOM gave an alternate vertical-horizontal polarization; *A* was a linear polarizer while *B* was absent. In all of these schemes, the intensity modulation of the probe beam was lock-in detected.

Atomic oxygen was produced using an electrodeless rf discharge [12]. The sample cell was a 5-mm-diameter Pyrex tube; because of the high chemical reactivity of

atomic oxygen, it was impossible to use sealed-off cells. In fact, the concentration of oxygen during the operation of the discharge was observed to change rapidly due to the adsorption in the pyrex walls or reaction with other chemical species produced in the discharge itself. As a consequence, it was necessary to connect the sample cell to a vacuum and gas handling system (diffusion pump with a liquid nitrogen trap), which allowed us to easily change the gas mixture in the cell. The residual pressure in the cell before introducing the gas was less than 10^{-5} Torr. O_2 -Ar mixtures were used in this experiment. A typical O_2 -to-Ar pressure ratio was 1/20 and sub-Doppler signals could be detected for total pressure ranging from about 1 down to 10^{-3} Torr. For the measurement of the hyperfine structure and isotope shift, a 50% ^{17}O - ^{18}O -enriched sample was used. Natural abundances are $^{17}\text{O} = 0.04\%$, $^{18}\text{O} = 0.2\%$, and the enriched sample enhances the relative signal sizes.

As mentioned above, the shape of the lines observed by velocity-selective optical pumping can be influenced by the presence of magnetic fields. For a better definition of this parameter and to be able to choose the direction of the field, a pair of Helmholtz coils was used. The diameter of the coils was 25 cm and fields up to 3 G were produced in the central region. The small dimensions of the discharge ($\sim 0.5 \text{ cm}^3$) allowed a good uniformity of the field over the interaction region.

IV. RESULTS AND DISCUSSION

A. Observed line shapes

In Sec. II we have discussed the possible effects of VCC on the shape of the sub-Doppler lines. In particular, we have mentioned as different profiles can be expected depending on the particular observable investigated and on the cross section for atomic depolarization or de-excitation in collisions. In Fig. 3(a) we show the spectrum of the $3s^5S_2 - 3p^5P_3$ transition as obtained by saturation spectroscopy. As expected from the theory, the saturation line shape can be well approximated with the sum of a Lorentzian peak and a Gaussian background [Eq. (1)]; this had already been observed in Ref. [13], where sub-Doppler spectra for different transitions of atomic oxygen had been investigated by means of intermodulated optogalvanic spectroscopy.

The different effect of collisions on orientation and alignment is qualitatively evident from a comparison of the spectra shown in Figs. 4 and 5. In fact, the line shape of Fig. 4(a), recorded by velocity-selective orientation, can still be approximated by the expression (1), but with respect to saturation spectra the collisional background has a reduced width ($\sim 600 \text{ MHz}$), which indicates the presence of velocity-changing collisions of intermediate strength [Fig. 4(b)]. In the alignment line shape (Fig. 5), on the contrary, the contribution of the collisional background is absolutely negligible, and the experimental profile is well fitted by a pure Lorentzian [$C \sim 0$ in Eq. (1)]. This observation demonstrates that orientation and alignment have very different lifetimes in our experimental conditions. It can be due to the fact that the two ob-

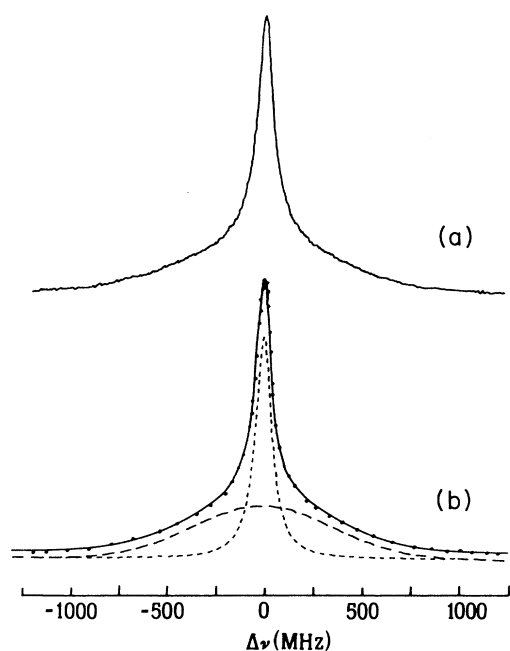


FIG. 3. Saturation spectroscopy of the $J=2 \rightarrow J'=3$ transition at 777.4 nm. In (a) the experimental line shape is shown, recorded in a cell containing a 1:10 O₂-Ar mixture at a total pressure of 1.4 Torr with a power of 1 mW of the pump beam. In (b) the profile is fitted with the sum of a Lorentzian homogeneous signal and a Gaussian background due to the velocity-changing collisions. The width of the pedestal is 1270 MHz and its relative amplitude is $C=0.24$.

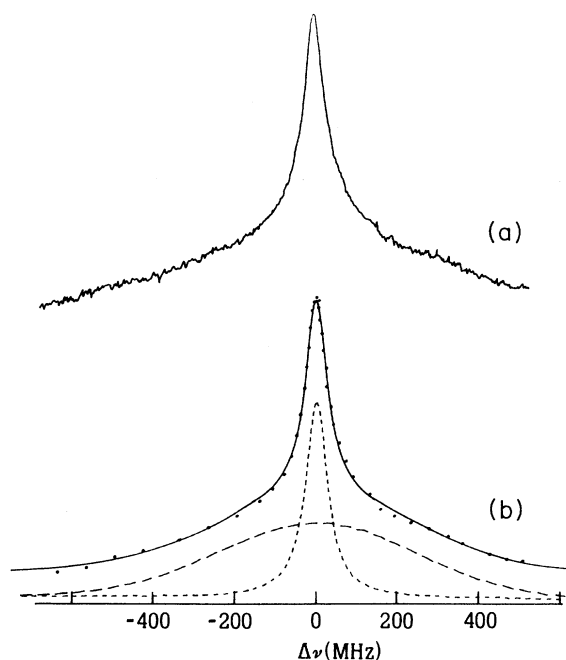


FIG. 4. The same transition of Fig. 3 as observed using velocity-selective orientation detection. In this case the width of the pedestal is 580 MHz while $C=0.37$.

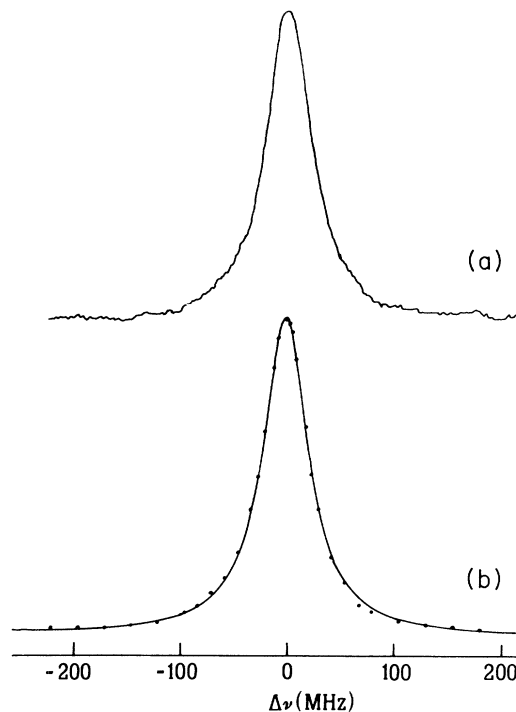


FIG. 5. A pure Lorentzian profile ($C \sim 0$) is recovered when velocity-selective alignment detection is adopted. Atoms undergoing velocity-changing collisions get depolarized and do not contribute to the signal.

servables have different depolarization cross sections for collisions with the buffer gas. This could also be explained by the presence in our experimental apparatus of a weak magnetic field along the sample cell. A longitudinal magnetic field tends to destroy the alignment and to preserve the orientation of atoms.

A reduction of the collisional pedestal in the orientation signal can be accomplished by applying a weak magnetic field to the sample in a direction perpendicular to the laser beams. In fact, Fig. 6 shows spectra recorded by velocity-selective orientation in the presence of a transverse magnetic field of increasing intensity. As explained in Sec. II, the magnetic field causes a precession of the oriented atoms and, as a consequence, leads to their depolarization. The process is more efficient for moving atoms which do not interact simultaneously with both the laser beams, i.e., atoms undergoing velocity-changing collisions while in the interaction region or atoms which, after leaving the interaction region, can return in it with a different velocity. The progressive reduction of the background intensity with increasing transverse field corresponds, indeed, to the increased depolarization of the atoms.

Also, the dependence of the sub-Doppler line shapes on the nature of the collisional partner was investigated. As mentioned in Sec. II, atoms in the 5S state cannot be disoriented in collisions with noble gases. In fact, Fig. 7 shows a comparison between two recordings of the same

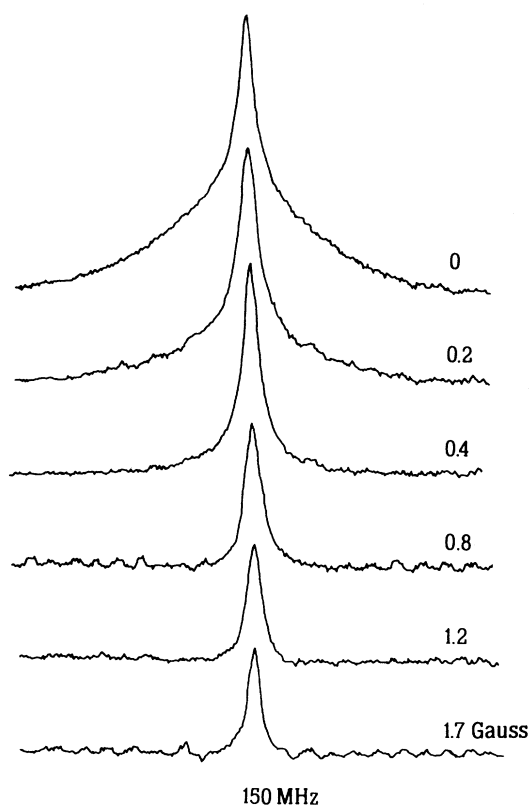


FIG. 6. Spectra recorded by velocity-selective orientation in presence of a weak magnetic field in the sample cell in a direction perpendicular to the laser beam.

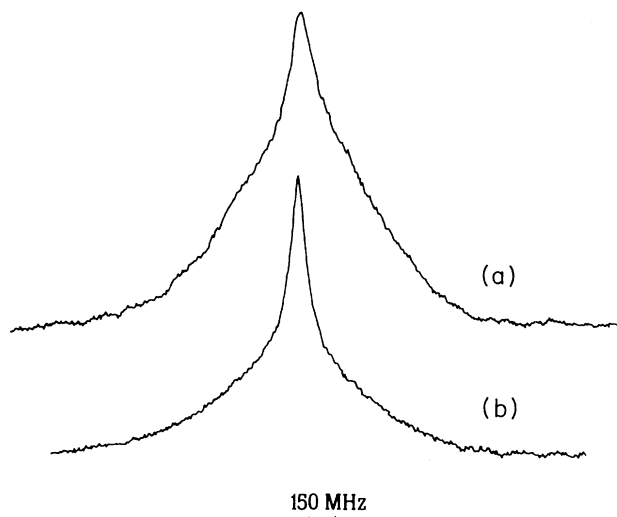


FIG. 7. Effect of the buffer gas on the profile of the $3^3S_2-3^3P_1$ transition observed by velocity-selective orientation detection. In (a) the sample cell contains 0.7 Torr of argon and oxygen is present only in trace amounts. In (b) the mixture contains 15% oxygen.

line, detected by velocity-selective orientation in discharges with different relative concentrations of oxygen in argon. It is evident in Fig. 7(a) that, when collisions with the buffer gas are dominant, the background almost obscures the sub-Doppler peak. On the contrary, in pure oxygen discharges Lorentzian line shapes could be observed. However, while the narrowing effect of the transverse magnetic field could be exploited in this work to increase the spectral resolution (see below), it was not possible to use discharges sustained by pure oxygen; in fact, in these conditions only weak signals were detected because of the inefficient dissociation of O_2 molecules.

From the results reported so far, we concluded that the velocity-selective alignment technique could allow an accurate measurement of the radiative linewidth of the investigated transition. The interest of such measurement stems from the fact that the $3p^5P_3$ -level lifetime plays a critical role in a scheme proposed for the cooling of atomic oxygen. A systematic analysis of the linewidth of the $3s^5S_2-3p^5P_3$ transition was performed for different pressures and laser power (Fig. 8). By extrapolating to both zero pressure and low laser power, a value for the radiative linewidth of 23 MHz was obtained, which corresponds to $\tau=7$ ns for the lifetime of the $3p^5P_3$ level (the decay rate of the lower metastable state does not contribute to the observed linewidth). The measured value of τ is within the favorable range for the realization of the experiment of cooling of atomic oxygen. Similar values for the radiative lifetime were obtained by extrapolating to zero pressure the linewidths measured with the other two techniques; however, the result obtained by the alignment detection is the most accurate, because of the absence of the collisional background in the recorded lines.

The situation is different when a hyperfine structure is present; in this case, a complication of the spectra resulted when velocity-selective alignment detection was adopted. In Fig. 9, the recorded spectra relative to the

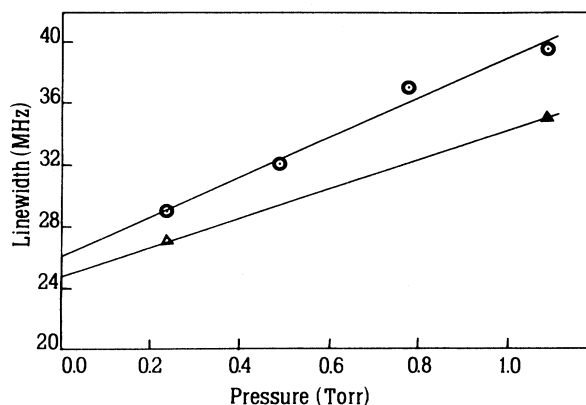


FIG. 8. Linewidth of the 777.7-nm line, recorded using the velocity-selective alignment scheme, as a function of the total pressure in the sample cell, for two different laser intensities (○: 2.2 mW, △: 0.9 mW).

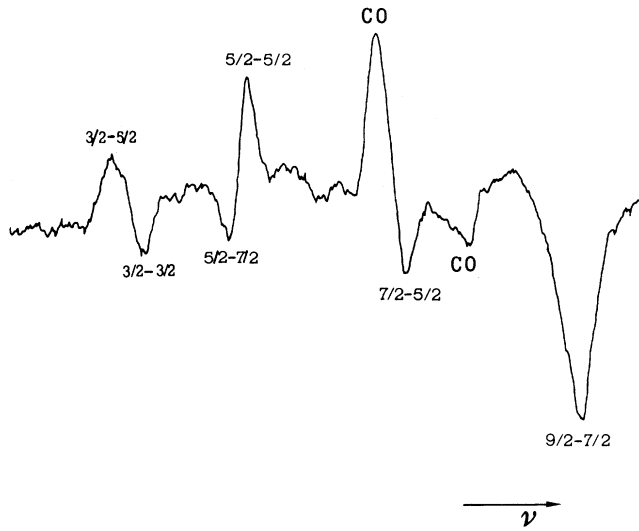


FIG. 9. Hyperfine structure of the 777.7-nm transition of ^{17}O , observed by velocity-selective alignment detection. CO denotes crossover signals.

hyperfine structure of the $3^5S_2-3^5P_1$ transition of ^{17}O is reported. Resonance peaks can have both positive and negative signs and many spurious signals, identifiable as crossover resonances, are present. So, in spite of the increased resolution offered by this technique in simple cases, it was not taken into account for the determination of the hyperfine structure of the 5S_2 level, as discussed in Sec. IV C.

B. Measurement of the fine structure of the $3p^5P_{1,2,3}$ level

The fine structure of the energy levels of atomic oxygen has been widely investigated, both by conventional [14] and high-resolution spectroscopy [13]. Its interest stems from the fact that various relativistic effects, not only the spin-orbit coupling, play a role. Accurate data are then useful to test theoretical models. In this work we measured the fine structure of the $3p^5P_{1,2,3}$ level.

As is clear from the level scheme shown in Fig. 1, the three fine-structure components of the $3^5S_2-3p^5P_{1,2,3}$ transition are too distant from each other (~ 60 GHz for the $J=1\leftrightarrow J=2$ and ~ 110 GHz for the $J=2\leftrightarrow J=3$ separations) to be observed in a single scan of the laser frequency. As a consequence, these splittings could not be measured by scanning the laser frequency and using the Fabry-Perot cavity for the frequency calibration, as we did for the smaller hyperfine splittings (see below). We exploited, then, the high accuracy (1 part in 10^7) of the λ meter to measure these separations as the difference of the frequency of optical transitions. The laser was locked to the zero of the first derivative of the saturation signal for each of the three transitions (see Sec. III). The wavelength was then measured by means of the λ meter. From the difference of the inverse of these values, the fine

structure separations were obtained. The results are $\Delta_{1,2}=60.56(15)$ GHz and $\Delta_{2,3}=110.18(15)$ GHz, in good agreement with the values 60.6 and 110.2 GHz respectively, reported in the literature as derived from conventional spectroscopy [15]. Ten measurements of the wavelength were taken for each of the lines; the values resulted all coincident within the significant digits given by the λ meter. In fact, considering the good signal-to-noise ratio (~ 100) of the saturation signal and the narrow linewidths (30–40 MHz) achieved in this experiment, the laser could be locked within ~ 400 kHz from the center of the line. The quoted errors correspond, then, to the accuracy offered by the λ meter. It is worth mentioning here that the demonstration of stable locking of the diode laser frequency to these resonances opens the possibility of performing a very accurate measurement of the isotope shift of this transition, by locking two lasers to the saturation signals of two different isotopes and beating them on a fast photodiode. As mentioned above, accurate measurements of the isotope shift are required to evidence volume effects on the spectra; the method just proposed could allow a further improvement in the accuracy of more than one order of magnitude with respect to the data reported in this paper (see next section).

C. Isotope shift and hyperfine structure

In Fig. 10 we show the spectra relative to the three fine-structure components of the 777-nm transition, recorded by saturation spectroscopy in an isotopically enriched sample. The transmission fringes of the 75-MHz free-spectral-range Fabry-Perot (not shown in the figure) were recorded simultaneously, which allowed an accurate frequency calibration. The ^{16}O - ^{18}O isotope shift can be immediately deduced from the spectra; averaging over several recordings, we determined a value of 1955(20) MHz. On the contrary, the isotope shift for ^{17}O is more difficult to evaluate because of the presence of the hyperfine structure. In the recordings shown in the figure, a major structure can be observed, formed by the five components corresponding to the hyperfine structure of the 5S_2 level ($I=\frac{5}{2}$). Each of the peaks, however, shows an underlying smaller structure deriving from the hyperfine structure of the 3^5P_J level; the higher the value of J , the more complex the spectrum. The final values for the hyperfine splittings were therefore taken from spectra relative to the $3^5S_2-3^5P_1$ transition, which has the simplest structure. The main cause of uncertainty on these values, in fact, derives from the unresolved hyperfine structure of the upper level. This also explains the only marginal agreement with the data reported in Ref. [1], which were obtained, instead, considering the $3^5S_2-3^5P_3$ transition. The homogeneous width of the lines and the presence of the collisional background prevent us from clearly resolving this structure. Using the technique of circular polarization modulation and applying a weak transverse magnetic field (0.5 G) to the sample (see Sec. IV A), we could go to lower pressures and reduce the background. As shown in Fig. 11, this allowed us to partially resolve the hyperfine structure of

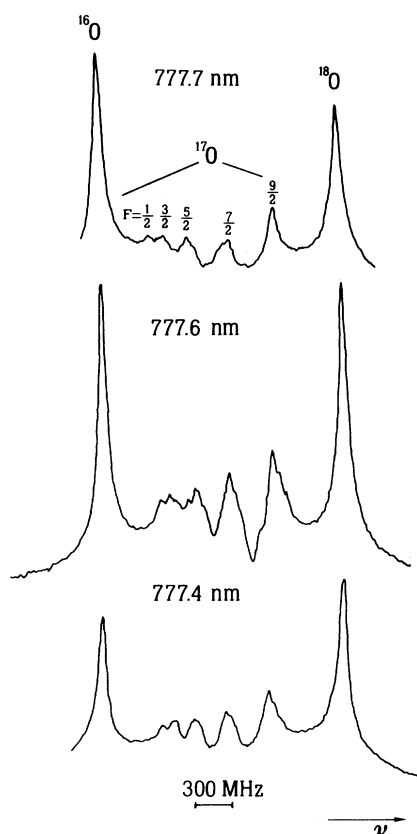


FIG. 10. Saturation spectroscopy of the three $3^5S_2-3^5P_J$ ($J=1,2,3$) transitions using an isotopically enriched sample. Five peaks are observed for ^{17}O , corresponding to the hyperfine structure of the 3^5S_2 level ($F=\frac{9}{2}, \dots, \frac{1}{2}$). Each of the five peaks shows a finer structure due to the upper state hyperfine splittings, which are only partially resolved.

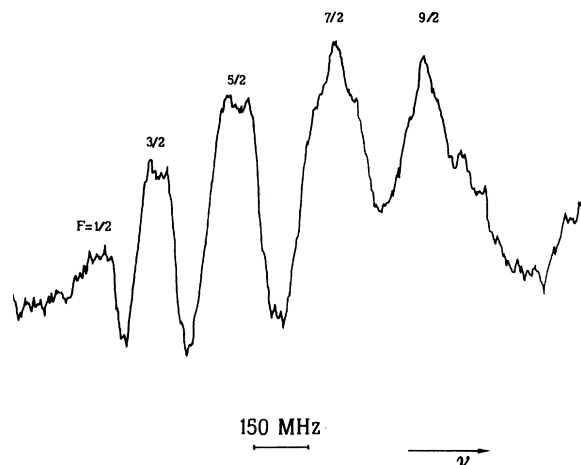


FIG. 11. The higher resolution achievable by the technique of velocity-selective orientation in the presence of a weak transverse magnetic field (0.7 G) allows to distinguish some of the components of the hyperfine structure of the 3^5P_2 level of ^{17}O .

the upper level of the transition, although the resolution is still too poor to provide reliable values for the separations. Only the data relative to the hyperfine splittings of the 5S_2 level are then reported in Table I; they were extracted from the spectra recorded by saturation spectroscopy and velocity-selective orientation, as just described. Data obtained by velocity-selective alignment, on the contrary, were not taken into account because of the higher complexity of the spectra.

From the data in Table I, several pieces of information on relevant physical quantities can be obtained. The measured energy splittings, in fact, can be fitted using the expression

$$E_F = E_J + \frac{1}{2}hAK + \frac{1}{4}hB[\frac{3}{2}K(K+1) - 2I(I+1)J(J+1)]/I(2I-1)J(2J-1) \quad (2)$$

with $K = F(F+1) - I(I+1) - J(J+1)$. The value obtained for the magnetic coupling constant A of the 5S_2 level is $A = -95(10)$ MHz. Also, from the observed structure of each of the five hyperfine components, the magnetic coupling constant A' of the 3^5P state can be estimated to be of the order of -30 MHz. The uncertainty affecting the value of the latter parameter does not allow us to give an estimate for the much smaller quadrupole coupling constant B . From the value of A , the electron density at the nucleus $|\Psi(0)|^2$ can be estimated. We obtain $\pi a_0^3 |\Psi(0)|^2 = 0.49(05)$, where a_0 is the Bohr radius.

Table II shows the results of the measurement of $^{16}\text{O}-^{18}\text{O}$ and $^{16}\text{O}-^{17}\text{O}$ isotope shifts. The $^{16}\text{O}-^{18}\text{O}$ isotope shift has been measured directly; the quoted error is essentially determined by the uncertainty in the calibration of the free spectral range of the Fabry-Perot interferometer. For the $^{17}\text{O}-^{18}\text{O}$ isotope shift, on the contrary, the center of gravity of the observed hyperfine structure

was considered. In this case then, the incomplete resolution of the 3^5P hyperfine structure is the main cause of uncertainty. The table also reports the separation between the ^{18}O peak and the transition of ^{17}O starting from the $I = \frac{9}{2}$ level of the 3^5S_2 state and reaching the

TABLE I. Hyperfine splittings $\Delta_{F,F'}$ (in MHz) of the 3^5S_2 level of ^{17}O obtained from the high-resolution investigation of the $3^5S_2-3^5P_1$ transition. Uncertainties correspond to one standard deviation.

$\Delta_{F,F'}$	Measured hf splittings (MHz)
$\Delta_{9/2,7/2}$	439 ± 15
$\Delta_{7/2,5/2}$	305 ± 10
$\Delta_{5/2,3/2}$	260 ± 12
$\Delta_{3/2,1/2}$	133 ± 9

TABLE II. Measured isotope shifts for the three stable isotopes of oxygen. The value for ^{17}O was determined considering the center of gravity of the hyperfine structure and the distance of the $I = \frac{9}{2} - I' - \frac{7}{2}$ component from the ^{18}O peak (also reported in the table).

$^{16}\text{O}-^{18}\text{O}$	$^{17}\text{O}-^{18}\text{O}$	$^{17}\text{O}_{(I=9/2-I'-7/2)}-^{18}\text{O}$
1955 ± 20	912 ± 20	485 ± 10

$I = \frac{7}{2}$ level of the $3p^5 P_1$ state. Because this line has no underlying structure, its position could be accurately measured.

The comparison of the IS values obtained in this work with those already measured for other transitions provides a further indication of the relevance of nuclear volume effects [16] in the spectrum of atomic oxygen, as already suggested in [2]. A deeper investigation of this interesting effect requires more accurate measurements of isotope shift and hyperfine structures. In fact, assuming a simple spherical nuclei model, the $^{16}\text{O}-^{17}\text{O}$ volume shift can be estimated to be about 1 MHz. This estimate is rather crude because it does not take into account the fact that the ^{16}O nucleus is “doubly magic.” However, it shows that the detection of the small effects we are searching for is at the limit of the possibilities of resolution. The experiment proposed in Sec. IV B for the measurement of the isotope shift by beating two lasers locked to the lines of two different isotopes could allow a dramatic improvement in the accuracy. Furthermore, in order to clearly evidence nuclear volume effects, it is necessary to dispose of accurate data for at least three different isotopes. This implies the complete resolution of the hyperfine structure of the $3^5 P_J$ levels of ^{17}O . We believe that the accuracy of the results reported in this paper for the hyperfine structure measurement can hardly be improved, unless completely new spectroscopic schemes are adopted. An interesting possibility can be represented, for example, by an experiment of radio-frequency-optical double resonance, as already demonstrated in hydrogen [17]. A simplification of the spectra

can also be achieved by investigating transitions of the triplet system of oxygen. The techniques developed in this work could then be immediately extended, for example, to the study of the $3^3 S_1 - 3^3 P_{1,2,0}$ transition which is in a spectral region (845 nm) reachable by diode lasers.

V. CONCLUSIONS

We have compared different spectroscopic techniques and optimized the experimental parameters to resolve the hyperfine structure of the $3^5 S_2 - 3^5 P_{1,2,3}$ transitions. Accurate values were obtained for the hyperfine splittings of the $3^5 S_2$ level, which allow us to give an estimate of the magnetic coupling constant A . This result is of great interest for a deeper understanding of nuclear effects on the atomic spectra. Since in light atoms these effects are difficult to detect, a further improvement in the accuracy of hyperfine structure and isotope-shift measurements is desirable. The proposed experiment of isotope-shift measurement by beating two lasers locked on different isotopes signals and a radio-frequency optical-double-resonance measurement of hyperfine structure appear very promising.

Furthermore, the high sensitivity achieved in this experiment and the versatility of diode lasers as high-spectral purity radiation sources, could allow an extension of these measurements to the unstable ^{15}O atom. In addition to the intrinsic interest of such an experiment, data relative to another isotope would increase the significance of data analysis methods, such as King plots [18], which allow us to extract information on nuclear parameters from the atomic spectra.

ACKNOWLEDGMENTS

The authors are indebted to L. Hollberg and R. Drulinger for exchange of information on the new laser source and to M. Pinard for fruitful discussions and critical reading of the manuscript. The authors also acknowledge suggestions by L. Zink for locking of the lasers to atomic lines. L. J. thanks the Scuola Normale Superiore di Pisa for financial support for her visit.

*Permanent address: Dipartimento di Scienze Fisiche dell'Università di Napoli, Napoli, Italy.

†Also at Dipartimento di Fisica, Università di Firenze, Firenze, Italy.

‡On leave from Laboratoire de Spectroscopie Hertzienne de l'ENS, Université Pierre et Marie Curie, Paris, France.

§Also Scuola Normale Superiore di Pisa, Pisa, Italy.

- [1] G. M. Tino, L. Hollberg, A. Sasso, M. Barsanti, and M. Inguscio, *Phys. Rev. Lett.* **64**, 2999 (1990).
- [2] L. Gianfrani, A. Sasso, G. M. Tino, and M. Inguscio, *Opt. Commun.* **78**, 158 (1990).
- [3] N. Kwon, M. Bohmolec, M. J. Colgan, and D. E. Murnick, *Phys. Rev.* **42**, 4408 (1990).
- [4] A. Sasso, M. I. Schisano, G. M. Tino and M. Inguscio, *J. Chem. Phys.* **93**, 7774 (1990).

- [5] M. Pinard, C. G. Aminoff, and F. Laloe, *Phys. Rev. A* **19**, 2366 (1979).
- [6] L. Julien, M. Pinard, and F. Laloe, *J. Phys. Lett.* **41**, L479 (1980).
- [7] C. Cohen-Tannoudji and A. Kastler, *Prog. Opt.* **5**, 1 (1966).
- [8] P. Bender, Thesis (Princeton University, Princeton, 1956).
- [9] P. W. Smith and T. Hansch, *Phys. Rev. Lett.* **26**, 740 (1971); C. Bréchnac, R. Vetter, and P. R. Berman, *Phys. Rev. A* **17**, 1609 (1977).
- [10] L. Julien, J. P. Descoubes, and F. Laloe, *J. Phys. B* **12**, L769 (1979).
- [11] C. G. Aminoff and M. Pinard, *J. Phys.* **43**, 263 (1982).
- [12] A. Sasso and G. M. Tino, M. Inguscio, N. Beverini, and M. Francesconi, *Nuovo Cimento* **10**, 941 (1988).

- [13] M. Inguscio, P. Minutolo, A. Sasso, and G. M. Tino, *Phys. Rev. A* **37**, 4056 (1988).
- [14] R.-J. Champeau, J. Jocotton, and E. Luc-Koenig, *J. Phys. B* **8**, 728 (1975).
- [15] K. B. S. Eriksson and H. B. S. Isberg, *Ark. Fys.* **24**, 549 (1963).
- [16] J. Bauche and R.-J. Champeau, *Adv. At. Mol. Phys.* **12**, 39 (1976).
- [17] E. W. Weber and J. E. M. Goldsmith, *Phys. Rev. Lett.* **41**, 940 (1978).
- [18] W. H. King, *Isotope Shifts in Atomic Spectra* (Plenum, New York, 1984).